A Journal of the Gesellschaft Deutscher Chemiker

Angewandte International Edition GDCh Chemie

www.angewandte.org

Accepted Article

Title: Probing the Paradigm of Promiscuity for N-Heterocyclic Carbene Complexes and their Protein Adduct Formation

Authors: Matthew P. Sullivan, Monika Cziferszky, Iogann Tolbatov, Dianna Truong, Davide Mercadante, Nazzareno Re, Ronald Gust, David C. Goldstone, and Christian Hartinger

To be cited as: *Angew. Chem. Int. Ed.* 10.1002/anie.202106906

Link to VoR: https://doi.org/10.1002/anie.202106906

WILEY-VCH

10.1002/anie.202106906

WILEY-VCH

RESEARCH ARTICLE

Probing the Paradigm of Promiscuity for *N*-Heterocyclic Carbene Complexes and their Protein Adduct Formation

Matthew P. Sullivan,[a,b] Monika Cziferszky,[c] Iogann Tolbatov,[d] Dianna Truong,[a] Davide Mercadante,[a] Nazzareno Re,[e] Ronald Gust,[c] David C. Goldstone,[b] and Christian G. Hartinger*[a]

[a] Dr. M. P. Sullivan, D. Truong, Dr. D. Mercadante, Prof. C. G. Hartinger*
School of Chemical Sciences
University of Auckland
Private Bag 92019, Auckland 1142, New Zealand
E-mail: c.hartinger@auckland.ac.nz; http://hartinger.auckland.ac.nz
[b] Dr. M. P. Sullivan, Dr. D. C. Goldstone
School of Biological Sciences
University of Auckland
Private Bag 92019, Auckland 1142, New Zealand
[c] Dr. M. Cziferszky, Prof. R. Gust
Department of Chemistry and Pharmacy
University of Innsbruck
Innrain 80/82, A-6020 Innsbruck, Austria
[d] Dr. I. Tolbatov
Institut de Chimie Moleculaire (ICMUB)
Université de Bourgogne Franche-Comté (UBFC)
Avenue Alain Savary 9, Dijon, France
[e] Prof. N. Re
Dipartimento di Farmacia
Università "G d'Annunzio" di Chieti - Pescara
Via dei Vestini 31, Chieti, Italy

Supporting information for this article is given via a link at the end of the document.

Abstract: Metal complexes can be considered a 'paradigm of promiscuity' when it comes to their reactions with proteins. They often form adducts with a variety of donor atoms in an unselective manner. We have characterized the adducts formed between a series of isostructural *N*-heterocyclic carbene (NHC) complexes with Ru, Os, Rh, and Ir centers and the model protein hen egg white lysozyme by X-ray crystallography and mass spectrometry. Distinctive behavior for the metal compounds was observed with the more labile Ru and Rh complexes targeting a surface L-histidine moiety through cleavage of *p*-cymene or NHC co-ligands, respectively. In contrast, the more inert Os and Ir derivatives were detected in an electronegative binding pocket after undergoing ligand exchange of a chlorido ligand for an amino acid side chain. Computational studies supported the binding profiles and hinted at the role of the protein microenvironment for metal complexes eliciting selectivity for specific binding sites on the protein.

Introduction

Metal co-factors in enzymes are often essential to fulfil the biological function of a protein as a bio-catalyst. Consequently enzymes have evolved to host specific metal co-factors selectively attached in their active sites.[1] In contrast, anticancer metallodrugs are seen as promiscuous, *e.g.*, cisplatin primarily targets DNA[2] but was also shown to interact with serum proteins[3] prior to reaching DNA.[4] Such interactions have been considered to contribute to the side effects, while in the case of the clinically investigated Ru^{III} complex sodium [*trans*-tetrachloridobis(1*H*-indazole)ruthenate(III)] (KP1339/IT-139/BOLD-100) protein interactions are considered essential in its mode of action.[5] However, their intrinsic promiscuity makes the design of metal-based drugs that are selective for a protein target or even a single amino acid on a protein target a significant challenge. Generally, applicable design principles for metal complexes that enable the promiscuity to be controlled, so that they can act as effective metal-based protein co-factors with site-selective bond formation to the target protein, remain elusive despite proposed approaches to achieve selectivity.[6]

In the quest for alternative, more effective anticancer agents, half-sandwich organoruthenium compounds were investigated, and small structural changes result in complexes targeting protein or DNA, and differing biological activity.[7]

We recently reported congeneric *N*-heterocyclic carbene complexes to the protein-targeting [Ru(arene)(1,3,5-triaza-7-phosphaadamantane)X_2] (RAPTA) compounds with the formula [M(L)(dmb/dbb)Cl_2] (Figure 1; M = Ru/Os/Rh/Ir; L = η^6-*p*-cymene [cym], η^5-pentamethylcyclopentadienyl [Cp*]; dmb = 1,3-dimethylbenzimidazol-2-ylidene; dbb = 1,3-dibenzylbenzimidazol-2-ylidene),[8] which showed thioredoxin reductase (TrxR) inhibitory activity. [Rh(Cp*)(dbb)Cl_2] was the most potent cytotoxic agent of the series, and also inhibited TrxR most effectively. We demonstrated the crucial role of the Rh center as the Rh(dmb) analogue also inhibited TrxR despite showing lower antiproliferative activity.[8c]

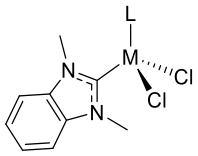

1 M = Ru **L** = cym
2 M = Os **L** = cym
3 M = Rh **L** = Cp*
4 M = Ir **L** = Cp*

Figure 1. General structure of dmb complexes of Ru-, Os(cym), Rh-, and Ir(Cp*).

Inspired by the differing biological properties of the isostructural compounds,[9] seemingly driven by the metal center, we investigated the implications of altering the metal center in [M(L)(dmb)Cl_2] complexes on the interactions with the model protein hen egg white lysozyme (HEWL) using protein crystallography and electrospray ionization (ESI)-MS. In addition, the results were rationalized with *in silico* molecular modelling and dynamics studies to analyze the interaction profiles of the congeners on HEWL.

Results and Discussion

In preliminary studies, we have shown that [Ru(cym)(dmb)Cl_2] **1** mainly interacts with HEWL through coordination to $N^{\varepsilon1}{}_{His15}$ and binding was concomitant with the loss of the cym ligand, formation of a bifunctional adduct through additional coordination to $N^{\eta1}{}_{Arg14}$ and oxidation of the Ru center (Figure 2a).[10] To investigate the impact of the metal center of isostructural compounds on protein metalation, we investigated the binding of HEWL to **2**–**4** (Figure 1).

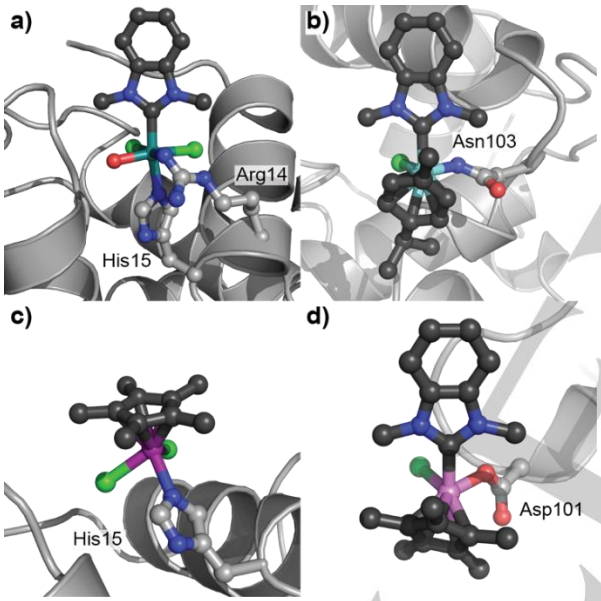

Figure 2. Details of the primary binding sites for **1**–**4** on HEWL. All adducts and binding sites are indicated in ball and stick representation with the Ru (**1**, deep teal), Os (**2**, aquamarine), Rh (**3**, purple), and Ir (**4**, violet) centers highlighted. a) bifunctional adduct of [Ru(dmb)(H_2O)Cl_2] with His15 and Arg14; b) [Os(cym)(dmb)Cl] adduct with Asn103; c) monodentate interaction of His15 with [Rh(Cp*)Cl_2]; d) [Ir(Cp*)(dmb)Cl] conjugated to Asp101.

For the Os compound **2**, three metalation sites were found with the most prominent at the $N^{\delta1}{}_{Asn103}$ atom with an Os–N distance of 2.10 ± 0.04 Å. The adduct featured π-bound cym, chlorido, and NHC ligands at the Os center with an occupancy of 0.8 for the whole fragment, which is lower than that observed for the fragment derived from **1** (Figures 2b and S1, Table S1). In contrast to the adduct of **1**, the more inert Os complex maintained the pseudo-octahedral coordination geometry, typical of piano-stool complexes. A secondary binding site with a 25% occupancy was observed at $O^{\delta1}{}_{Asp18}$, however, no ligands could be accurately assigned (Figure S2). Another molecule of **2** was found to form π-stacking interactions with Trp123 and possibly H bonding with Lys33 and/or Arg5 (Figure S3), while retaining all its original ligands.

To compare the interactions of the M^{II}(cym) complexes **1** and **2** with those of the M^{III}(Cp*) complexes **3** and **4**, the HEWL binding of the latter compounds was investigated under the same conditions. Similar to the Ru derivative **1**, the main binding site of **3** was found at His15 (Figures 2c and S4, Table S1) but the Cp* ligand was retained at the Rh center and instead the NHC moiety was substituted with $N^{\varepsilon1}{}_{His15}$. Overall, the fragment had an occupancy of 0.9, with a Rh–$N^{\varepsilon1}{}_{His15}$ distance of 2.22 ± 0.04 Å, which is longer than the Ru–N bond length in the HEWL–**1** adduct (2.13 Å).[10] A second site was disordered with regard to the Asp101 side chain, resulting in modelling of the adduct at one of the two conformers (0.5 occupancy). The binding occurred through $O^{\varepsilon2}{}_{Asp101}$ (Figure S5) after exchange of a chlorido ligand of **3**, while the NHC moiety remained coordinated to the Rh center. The Ir^{III} complex **4**, as the more inert analogue of **3**, formed a single [Ir(Cp*)(dmb)Cl] adduct at Asp101 with an Ir–$O^{\varepsilon2}{}_{Asp101}$ distance of 1.95 ± 0.05 Å (Figures 2d and S6, Table S1) at an occupancy of 0.5, notably lower than found for any of the fragments of **1**–**3**.

Overall, there were distinctive differences observed for the interactions of the metal complexes with HEWL at the most prominent sites. The Ru (**1**) and Rh (**3**) compounds interacted with the $N^{\varepsilon1}{}_{His15}$ atom, however, they underwent distinct changes in their structures upon binding to the protein, with the cleavage of the cym and NHC ligands, respectively. The heavier congeners **2** (Os) and **4** (Ir) underwent chlorido ligand substitution with an amino acid side chain donor atom, *i.e.*, $N^{\delta1}{}_{Asn103}$ and $O^{\delta1}{}_{Asp101}$, respectively. The adducts of the latter compounds were detected in the electronegative peptidoglycan-binding pocket of the protein (Figure 3, site 2). Note that the secondary binding site for **3**, in which a chlorido ligand was exchanged for Asp101, follows the same trend as for **2** and **4**. This behavior can be explained by the different formation rates of aqua intermediates in aqueous solution,[8b] and consequently of complex cations allowing for Coulomb interactions with HEWL. Compounds **1** and **3** formed immediately mixtures of chlorido/aqua species and the addition of $AgNO_3$ induced the formation of the diaqua complexes, while **2** and **4** were more stable (Figures S7–S10). Notably, complexes **1** and **3,** which underwent substantial changes with the cym and NHC ligand substituted for amino acid side chains, were found in electropositive sites on the protein surface (sites 1 and 3 for **1** and **3**; Figure 3).

10.1002/anie.202106906

RESEARCH ARTICLE

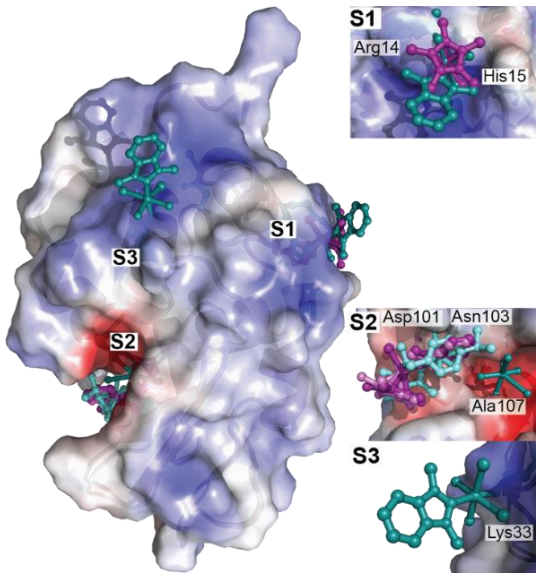

Figure 3. Locations of the significant binding sites of **1** (deep teal), **2** (aquamarine), **3** (purple), and **4** (violet) on an electrostatic surface[11] of HEWL. Red and blue regions indicate electronegative and electropositive areas. Site 1 (S1) features fragments of **1** and **3** interacting with His15, whereas site 2 (S2) contains fragments of **4** interacting with Asp101 (as well as of **3**) and of **2** with Asn103. Site 3 (S3) features a fragment of **1** bound to Lys33.

Top-down MS has been shown to be capable of identifying binding sites of metal-based drugs on biomolecules.[12] To complement the data obtained by crystallography, top-down MS studies were conducted for adducts formed between HEWL and **1**–**4**. Adducts of the type [HEWL + M(cym/Cp*)(dmb)Cl_n]$^+$ (n = 0, 1) were detected upon incubation of the metal complexes and HEWL (Figure 4 for **2,** Table S2). Attempts to directly fragment metal-containing HEWL species failed. However, reduction of the disulfide bonds in HEWL by TCEP·HCl resulted in higher charge states and higher-energy collisional dissociation (HCD) spectra without altering the metal-binding pattern, as demonstrated for **2** (Figure 4). In case of the reaction between HEWL and **1**, the binding site was identified as His15 through the presence of several b fragments in the tandem mass spectrum, including [b27 + Ru(cym)(dmb)] (Table S3). In the top-down MS experiments, Ru retained its cym ligand, which can be explained by shorter incubation periods and different conditions compared to the crystal soaking experiments. For the reaction between **2** and HEWL, a number of b fragments containing an Os(cym)(dmb) moiety were identified (Table S4), including b28 and b30-33 indicating a binding site in the *N*-terminal region, possibly Asp18 as identified by protein crystallography. The C-terminal fragment [y81 + Os(cym)(dmb)] had low abundance in charge states +8 and +9 and was the only MS-based confirmation of Asn103 as a binding site for **2**. Complex **3** formed the low abundant adduct [HEWL + Rh(Cp*)], where the NHC ligand is absent, confirming the crystallography data. HCD fragmentation of the reduced adduct led to the cleavage of the Rh moiety and no Rh-containing fragments could be detected. The observation of weaker interactions between the protein and Rh correlates to the elongated Rh–$N^{\varepsilon1}_{His15}$ distance compared to Ru–$N^{\varepsilon1}_{His15}$ in the protein crystal structure. Reduction of the Ir adduct [HEWL + Ir(Cp*)(dmb)] with TCEP·HCl resulted in loss of the adduct signal and the emergence of *m/z* 723.22, corresponding to [Ir(Cp*)(NHC)(TCEP) – H]$^+$, which demonstrated the phosphine mediated cleavage of Ir from the protein, and also the limitation of the method. However, overall the protein crystallographic studies could largely be confirmed by mass spectrometry experiments.

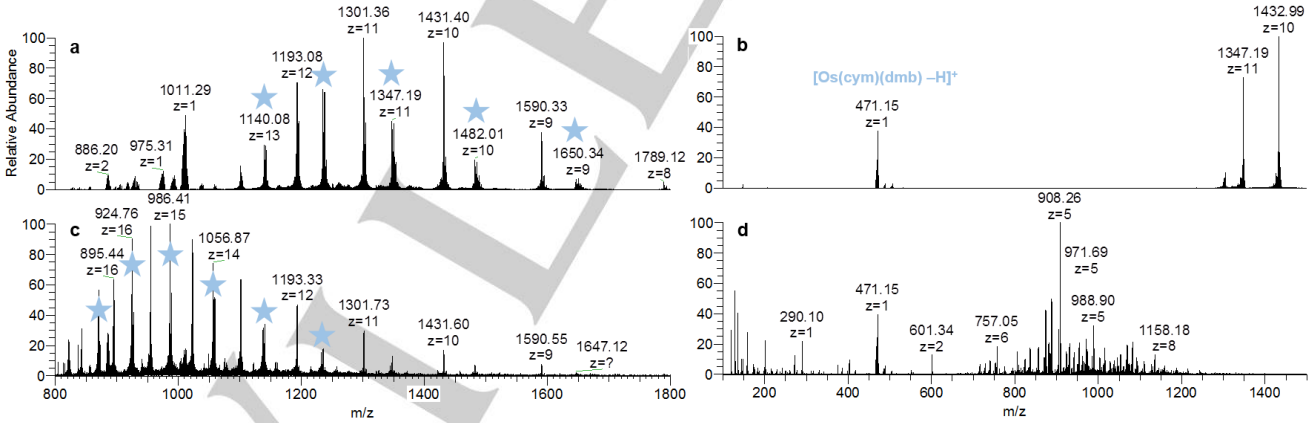

Figure 4. Mass spectra of HEWL and **2**. a) Full spectrum of HEWL after 10 days of incubation with 10 eq. of **2**. Blue stars mark Os-containing HEWL species. b) HCD fragmentation of HEWL leads to loss of the metal fragment only. c) Reduction of disulfide bonds resulted in higher charge states and d) fragmentation to allow for binding site characterization.

With the aim of elucidating the molecular basis of these observations, protonation tendencies of reactive amino acids and thermodynamics of bond-dissociation for the organometallic compounds were further investigated by *in silico* methods spanning constant-pH molecular dynamics (CpHMD) simulations and DFT calculations. While crystallographic evidence suggests a higher occupancy for positively charged sites, the reactivity of certain acidic residues over others is less clear. CpHMD simulations estimated canonically predictable protonation behaviors for His15 and Lys33 with a large solvent exposure leading to pK_a values of 6.67 and 9.91, respectively. Notably, the calculations suggest significant differences between the deprotonation tendencies of Asp87 and Asp101 (Figure S11) with the calculated pK_a values being 2.73 and 0.44. Overall, this indicates significantly different populations of carboxylate moieties, for example Asp87 is in close proximity to His15 and take part in a hydrogen-bonding network, which suggests a coupled Asp87-His15 protonation. This is evidenced by the pK_a

shift of fully solvent exposed Asp87 to approximately 1.3 pH units lower than found for solvent-exposed Asp (pK_a = 4). This is likely to affect the electropositivity of His15, providing insights into the observed specificity for **1** and **3** rather than **2** and **4**, which preferentially bind to an electronegative binding pocket even though His15 is available as a targetable site. The hydrogen bond network also orients $N^{\varepsilon 1}{}_{His15}$ towards the solvent, likely explaining the observed binding preference.

DFT calculations of the bond-dissociation Gibbs free energies (BDFE) affecting the coordinative bonds in the complexes were performed to rationalize the different ability of the piano-stool complexes in targeting protein residues (Table 1).

Table 1. Bond-dissociation free energy values (BDFE) of the coordinative bonds in complexes **1**-**4** (Gibbs free energy, kcal/mol).

Complex	Gibbs free energy, kcal/mol			
	M–Cl	M–dmb	M–cym	M–Cp*
1 (Ru)	31.1	30.1	28.3	-
2 (Os)	31.4	33.8	50.2	-
3 (Rh)	25.8	25.5	-	132.1
4 (Ir)	25.7	31.2	-	143.2

The bond-dissociation free energy value calculations confirmed that the negatively charged Cp* ligands are strongly bound to the Rh and Ir centers, with BDFE values of 132.1 and 143.2 kcal/mol, respectively. The coordination of the cym ligands to Ru and Os is significantly weaker, with BDFE values of 28.3 and 50.2 kcal/mol, respectively (Table 1). The BDFE values of both the chlorido and dmb ligands were detected in a narrow range of 25–34 kcal/mol, indicating a similar bond strength. Notably, the M–Cl and M–dmb bonds are approximately 3–5 kcal/mol stronger when M = Ru or Os. The DFT results are in good agreement with the observed binding pattern of **1**–**4** to HEWL, in particular with regard to the composition of the first coordination sphere detected upon long incubation times. The calculations predict the retention of the strongly bound Cp* ligand in **3** and **4**, whereas cym is more likely to be cleaved upon coordination to a protein side chain. Therefore, the release of the NHC ligand in **3** is consistent with the lower BDFE value observed, while the loss of the chlorido over the NHC ligand was slightly more favorable for **2** and **4**. The reaction free energies for the ligand substitution in **1**–**4** with side chains of His, Asp, and Asn residues were calculated by means of DFT calculations (Table S5). The substitution of the chlorido ligand by His or Asp side chains over Asn was found to be favorable in all complexes. This also supports the experimental observation that the substitution of dmb with His15 was more accessible in **1** and **3**, while the chlorido substitution in **2** and **4** by the carboxylato group of aspartate was found to be favorable by -4.5 and -4.1 kcal/mol, respectively (Table S5).

Conclusion

Inspired by the pharmacological activity of metal(NHC) complexes and the surprising reactivity of the Ru complex **1** with HEWL, we investigated the interactions of the isostructural Ru-, Os(cym), Rh-, and Ir(Cp*) complexes **1**–**4** with HEWL using protein crystallography, mass spectrometry and computational methods.

While the Ru complex **1** reacted more readily with His15/Arg14 and cym was cleaved, the Os congener **2** bound primarily to Asn103 of HEWL in a monofunctional manner. For the analogous Cp* complexes **3** and **4**, the $Rh(Cp^*)Cl_2$ fragment of **3** was found to substitute the NHC ligand for His15, whereas Ir-based **4** underwent chlorido/Asp101 ligand exchange and formed a monofunctional adduct. DFT calculations provided to some degree a rationalization of the experimental trends with regards to the chlorido ligand substitution by His or Asp side chains for **2** and **4**, whereas **1** and **3** release cym and dmb, respectively. The more labile Ru and Rh complexes preferentially bind to the His15 residue with high occupancy in the protein crystallographic experiments whereas the more inert compounds are attracted to the electronegative peptidoglycan-binding pocket, in particular, the Ir compound **4**. In addition, CpHMD simulations revealed different protonation tendencies for residues with similar solvent exposure.

The integrated investigation of structure-reactivity relationships by experimental and computational approaches provides a powerful tool for the rational design of compounds targeting specific areas on proteins. Our data suggests that the promiscuity of metal complexes can to some extent by controlled by considering the finely-tuned interplay between the microenvironment of the protein and the physicochemical properties specific to metal complexes. For further information on the crystallographic studies, mass spectrometry data, and computational work please refer to the Supporting Information.

Acknowledgements

We thank the Universities of Auckland and Innsbruck, the University of Auckland Faculty of Science Research and Development Fund, and the Cancer Research Trust NZ for financial support. This research was undertaken in part using the macromolecular crystallography beamlines (MX1 and MX2) beamlines at the Australian Synchrotron, part of ANSTO, and made use of the Australian Cancer Research Foundation (ACRF) detector. Constant-pH molecular dynamics simulations were performed using the GPU-equipped Nectar cloud infrastructure provided by the Center for eResearch of the University of Auckland (http://www.eresearch.auckland.ac.nz).

Keywords: Bioorganometallic chemistry • *N*-Heterocyclic carbene complexes • Protein mass spectrometry • Metal-protein interactions • Protein crystallography

[1] L. Banci, I. Bertini, in *Metallomics and the Cell* (Ed.: L. Banci), Springer Netherlands, Dordrecht, **2013**, pp. 1-13.

[2] B. Lippert, *Cisplatin: Chemistry and Biochemistry of a Leading Anticancer Drug*, Verlag Helvetica Chimica Acta, Zurich, **1999**.

[3] a) A. I. Ivanov, J. Christodoulou, J. A. Parkinson, K. J. Barnham, A. Tucker, J. Woodrow, P. J. Sadler, *J. Biol. Chem.* **1998**, *273*, 14721-14730; b) W. Hu, Q. Luo, K. Wu, X. Li, F. Wang, Y. Chen, X. Ma, J. Wang, J. Liu, S. Xiong, P. J. Sadler, *Chem. Commun.* **2011**, *47*, 6006-6008; c) G. Ferraro, L. Massai, L. Messori, A. Merlino, *Chem. Commun.* **2015**, *51*, 9436-9439.

[4] a) A. T. Yarnell, S. Oh, D. Reinberg, S. J. Lippard, *J. Biol. Chem.* **2001**, *276*, 25736-25741; b) H. Iijima, H. B. Patrzyc, J. B. Dawidzik, E. E. Budzinski, H. C. Cheng, H. G. Freund, H. C. Box, *Anal. Biochem.* **2004**, *333*, 65-71.

[5] a) M. Sulyok, S. Hann, C. G. Hartinger, B. K. Keppler, G. Stingeder, G. Koellensperger, *J. Anal. At. Spectrom.* **2005**, *20*, 856-863; b) S. Kapitza, M. Pongratz, M. A. Jakupec, P. Heffeter, W. Berger, L.

Lackinger, B. K. Keppler, B. Marian, *J. Cancer Res. Clin. Oncol.* **2005**, *131*, 101-110; c) N. Cetinbas, M. I. Webb, J. A. Dubland, C. J. Walsby, *J. Biol. Inorg. Chem.* **2010**, *15*, 131-145.

[6] H. J. Davis, T. R. Ward, *ACS Central Science* **2019**, *5*, 1120-1136.

[7] a) Z. Adhireksan, G. E. Davey, P. Campomanes, M. Groessl, C. M. Clavel, H. Yu, A. A. Nazarov, C. H. Yeo, W. H. Ang, P. Droge, U. Rothlisberger, P. J. Dyson, C. A. Davey, *Nat. Commun.* **2014**, *5*, 1-13; b) Y. K. Yan, M. Melchart, A. Habtemariam, P. J. Sadler, *Chem. Commun.* **2005**, 4764-4776.

[8] a) L. Oehninger, M. Stefanopoulou, H. Alborzinia, J. Schur, S. Ludewig, K. Namikawa, A. Munoz-Castro, R. W. Koster, K. Baumann, S. Wolfl, W. S. Sheldrick, I. Ott, *Dalton Trans.* **2013**, *42*, 1657-1666; b) N. Y. S. Lam, D. Truong, H. Burmeister, M. V. Babak, H. U. Holtkamp, S. Movassaghi, D. M. Ayine-Tora, A. Zafar, M. Kubanik, L. Oehninger, T. Söhnel, J. Reynisson, S. M. F. Jamieson, C. Gaiddon, I. Ott, C. G. Hartinger, *Inorg. Chem.* **2018**, *57*, 14427-14434; c) D. Truong, M. P. Sullivan, K. K. H. Tong, T. R. Steel, A. Prause, J. H. Lovett, J. W. Andersen, S. M. F. Jamieson, H. H. Harris, I. Ott, C. M. Weekley, K. Hummitzsch, T. Söhnel, M. Hanif, N. Metzler-Nolte, D. C. Goldstone, C. G. Hartinger, *Inorg. Chem.* **2020**, *59*, 3281-3289.

[9] a) A. Dorcier, W. H. Ang, S. Bolaño, L. Gonsalvi, L. Juillerat-Jeannerat, G. Laurenczy, M. Peruzzini, A. D. Phillips, F. Zanobini, P. J. Dyson, *Organometallics* **2006**, *25*, 4090-4096; b) M. P. Sullivan, M. Groessl, S. M. Meier, R. L. Kingston, D. C. Goldstone, C. G. Hartinger, *Chem. Commun.* **2017**, *53*, 4246-4249.

[10] M. P. Sullivan, M. K. Nieuwoudt, G. A. Bowmaker, N. Y. S. Lam, D. Truong, D. C. Goldstone, C. G. Hartinger, *Chem. Commun.* **2018**, *54*, 6120-6123.

[11] N. A. Baker, D. Sept, S. Joseph, M. J. Holst, J. A. McCammon, *Proc. Natl. Acad. Sci.* **2001**, *98*, 10037-10041.

[12] a) A. E. Egger, C. G. Hartinger, H. Ben Hamidane, Y. O. Tsybin, B. K. Keppler, P. J. Dyson, *Inorg. Chem.* **2008**, *47*, 10626-10633; b) A. Pratesi, C. Gabbiani, E. Michelucci, M. Ginanneschi, A. M. Papini, R. Rubbiani, I. Ott, L. Messori, *J. Inorg. Biochem.* **2014**, *136*, 161-169.

10.1002/anie.202106906

WILEY-VCH

RESEARCH ARTICLE

Entry for the Table of Contents

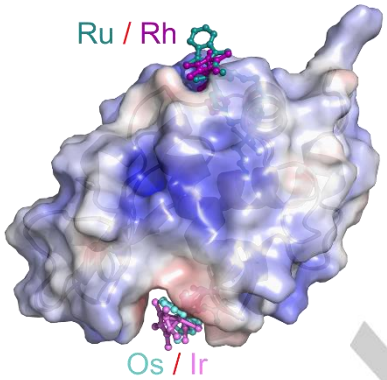

Isostructural *N*-heterocyclic carbene Ru, Os, Rh, and Ir complexes showed distinctive reactivity to hen egg white lysozyme by forming adducts at different binding sites and/or underwent different ligand exchange reactions. Protein crystallography, mass spectrometry and computational studies demonstrated the role of the metal centers and the protein microenvironment in determining their selectivity for a specific site.

Institute and/or researcher Twitter usernames: @HartingerHub, @matt_sullivan92, @DavideMercadan2, @CziferszkyLab